

A Microstructure and Hardness Study of Functionally Graded Materials Ti6Al4V/TiC by Laser Metal Deposition

REVIEWED

Jingwei Zhang¹, Yunlu Zhang¹, Frank Liou¹, Newkirk Joseph W², Karen M. Brown Taminger³, Walliam J. Seufzer³.

¹Department of Mechanical and Aerospace Engineering, Missouri University of Science and Technology

²Department of Materials Science & Engineering, Missouri University of Science and Technology

³NASA Langley Research Center, Hampton, VA 23681

Abstract

Crack free functionally graded material (FGM) Ti6Al4V-TiC has been fabricated by laser metal deposition (LMD) using TiC and Ti6Al4V powder which were premixed for different ratios. This study focuses on the influence of laser processing parameters and TiC compositional distribution on microstructure, Vickers hardness and phase. The microstructure is analyzed by scanning electron microscopy (SEM), x-ray diffraction (XRD) and hardness tests. Primary carbide, eutectic carbide and unmelted carbide are found in the deposit area. When laser power increased, the primary and secondary dendrite arm spacing increased. The laser power and scanning speed did not influence the Vickers hardness distribution significantly.

1 Introduction

Titanium alloys, especially the Ti6Al4V alloy, are widely utilized in aerospace industry, medical apparatus and manufacturing application. The reason is that Ti6Al4V possesses excellent properties, which includes high-strength-to-weight ratio, high temperature strength, low density and excellent corrosion resistance. However, Ti6Al4V doesn't have high surface hardness, stiffness or wear resistance, which limits Ti6Al4V application in some extreme conditions. Metal Matrix Composites (MMC) with ceramic reinforcements are often considered as candidates to improve mechanical, tribology and material properties. Liu et al.[1] investigated TiC/TA15 titanium matrix composite microstructure and room temperature tensile properties with different TiC volume fractions during laser melting deposition (LMD) process. The damage mechanism of the composites is dominated by particle cracking followed by ductile failure of the matrix. Candel et al. [2] proposed microstructure and tribological properties improvement of TiC particle reinforced Ti6Al4V MMC coatings on Ti6Al4V hot rolled samples with different addition of TiC and laser cladding (LC) process parameters during laser cladding process. Instead of room temperature, Liu et al.[3] researched laser melting deposited TiC/TA15 composite containing 10% TiC reinforcement at elevated temperature. Ochonogor et al. [4] developed titanium metal matrix composite to improve the hardness and wear resistant properties with different TiC percentage by laser cladding technique. Mahamood et al. [5] studied the

scanning velocity influence on microstructure, microhardness and wear resistance of laser deposited Ti6Al4V/TiC composite. However, when the TiC percentage rises, it is prone to form crack and high porosity owing to obvious discrepancy in coefficient of thermal expansion, ductility and toughness between Ti6Al4V and TiC. Functionally gradient materials (FGM) can be selected as one candidate to both improve material properties and build crack and pore free deposited parts. Liu and DuPont [6] developed crack-free functionally graded TiC/Ti materials by laser engineered net shaping (LENS) with compositions ranging from pure Ti to approximately 95 vol% TiC. F. Wang et al. [7] investigated building Ti6Al4V reinforced with TiC compositionally graded material by direct laser fabrication, microstructure and tribological properties. Obielodan and Stucker [8] focused on different designs of material transitions from Ti6Al4V alloy to Ti6Al4V/TiC composite and mechanical properties, such as tensile strength, yield strength and Young's modulus. In this work, microstructure, hardness and X-ray diffraction of a Ti6Al4V/TiC FGM part was investigated. Laser power and scanning speed variation influence on material properties are also discussed.

2 Experimental procedures

The raw materials used in this experiment are gas atomized Ti6Al4V powder mixed with varied volume percentage of TiC powder. The particle sizes of the Ti6Al4V spherical powder is between 125 μ m and 250 μ m, and TiC powder (99.5% purity) particle size is approximately from 45 μ m to 150 μ m. The substrate material is grade 5 Ti6Al4V alloy. Powder blends of TiC and Ti6Al4V with 10%, 20% and 30% TiC volume percentages were prepared for laser manufacturing the TiC/Ti6Al4V FGM part. Since the TiC powder was not gas atomized, the irregular TiC powder and Ti6Al4V spherical powder was mixed together before delivery in order to improve liquidity of powder delivery. The experiment was carried out with a 1kW Nd-YAG laser (IPG), a coaxial powder delivery nozzle and a computer controlled multiple axes translator. The two powders (Ti6Al4V and TiC powder) were dried in the furnace for 20 minutes at 180°C, then mixed for 30 minutes with TURBULA mixer and placed in a hopper of a powder feeder whose flow rate is directly proportional to the motor rotational speed. The laser beam diameter is approximately 2mm on the substrate surface. Argon gas was utilized to shield the substrate, mixed powder and deposit to prevent oxidization under high temperature. The deposition process was conducted by delivering the powder into the melt pool on the substrate and melting the powder with Nd:YAG laser. The substrate surface was ground with SiC abrasive paper and then degreased with alcohol prior to the LMD processes. The schematic of the laser deposition process is shown in Figure 1.

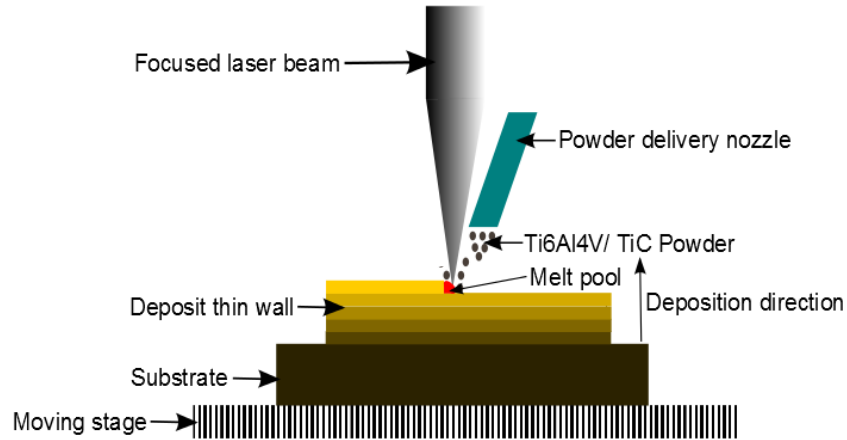


Figure 1. Laser Powder Deposition Schematic

Ti6Al4V hot rolled alloy was used as the substrates in this experiment, with 2 inch by 0.5 inch by 0.25 inch size. Laser power ranged from 400W to 700W, and the scanning speed varied from 200mm/min to 400mm/min. Therefore, the energy density for each sample was 40.0, 82.5, 55.0, 41.2 and 70.0 J/mm^2 . The laser process parameters are shown in Table 1. Specimens were cut, ground, polished and etched in order to do further microscope observation and material properties test. A FEI Helios NanoLab DualBeam SEM was used to observe the cross sectional microstructure. A DURAMIN tester was utilized to measure the deposits hardness along the titanium carbide composition gradient direction. A Philips MRD was used to do XRD analysis so that the phase information of deposit area can be obtained. Ti-6al-4V and TiC powder shape and size information is shown in Figure 2.

Table 1. Laser Processing Parameters

	Power(W)	Scanning Speed(mm/min)	Substrate Size	Energy density(J/mm^2)	Composition(volume%)
Sample 1	400	300	2"× 0.5"×0.25"	40.0	10%-20%-30%
Sample 2	550	200	2"× 0.5"×0.25"	82.5	10%-20%-30%
Sample 3	550	300	2"× 0.5"×0.25"	55.0	10%-20%-30%
Sample 4	550	400	2"× 0.5"×0.25"	41.3	10%-20%-30%
Sample 5	700	300	2"× 0.5"×0.25"	70.0	10%-20%-30%

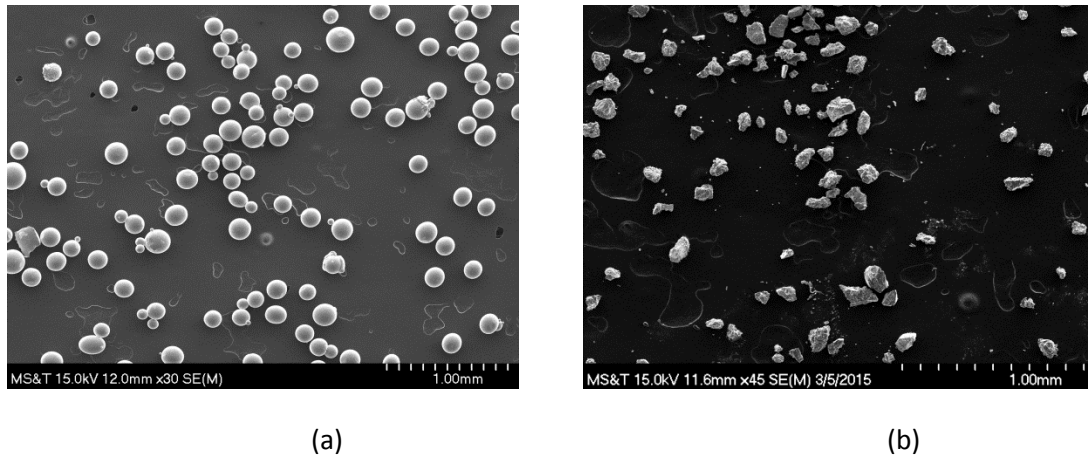


Figure 2. (a) Ti-6Al-4V powder SEM image (b) TiC powder SEM image

3 Results and Discussion

3.1 Microstructure

Figure 3 shows the microstructure of Ti-6Al-4V/TiC FGM deposit from the substrate to deposit top region. There is a variation in microstructure as titanium carbide percentage increases. The titanium carbide shape and size are substantially different from the original TiC powder, since the rapid cooling rate during the laser metal deposition process influences the solidified product. Based on the Ti-C binary phase diagram, the eutectic point temperature is about 1670°C and TiC will form as the primary phase and grow at first if the carbon at% is larger than 2%. For 10 vol% TiC mixed powder, the carbon atomic percentage is approximately 8%, which is higher than the eutectic point. When the carbon concentration in the remaining liquid phase decreases to the eutectic point, the TiC + β binary eutectic reaction occurs. When the cooling rate is high, nonequilibrium condition cause pseudo eutectic reaction occurring near the eutectic point, which forms eutectic carbide as shown in Figure 3(b) and Figure 3(c) [9]. In Figure 3(d), both primary carbide and eutectic carbide appear in the deposit area. When carbon percentage increases, the hypereutectic reaction occurs before the temperature drops to eutectic temperature. When carbon content increases continuously, the difference between the liquidus temperature and eutectic temperature becomes larger, which allows the primary carbide more time to grow. Therefore, the long primary dendrite carbide can be seen in Figure 3(e). At the top of the deposit, some unmelted blocky carbides remain because the heat input cannot completely melt or dissolve the high content titanium carbide powder.

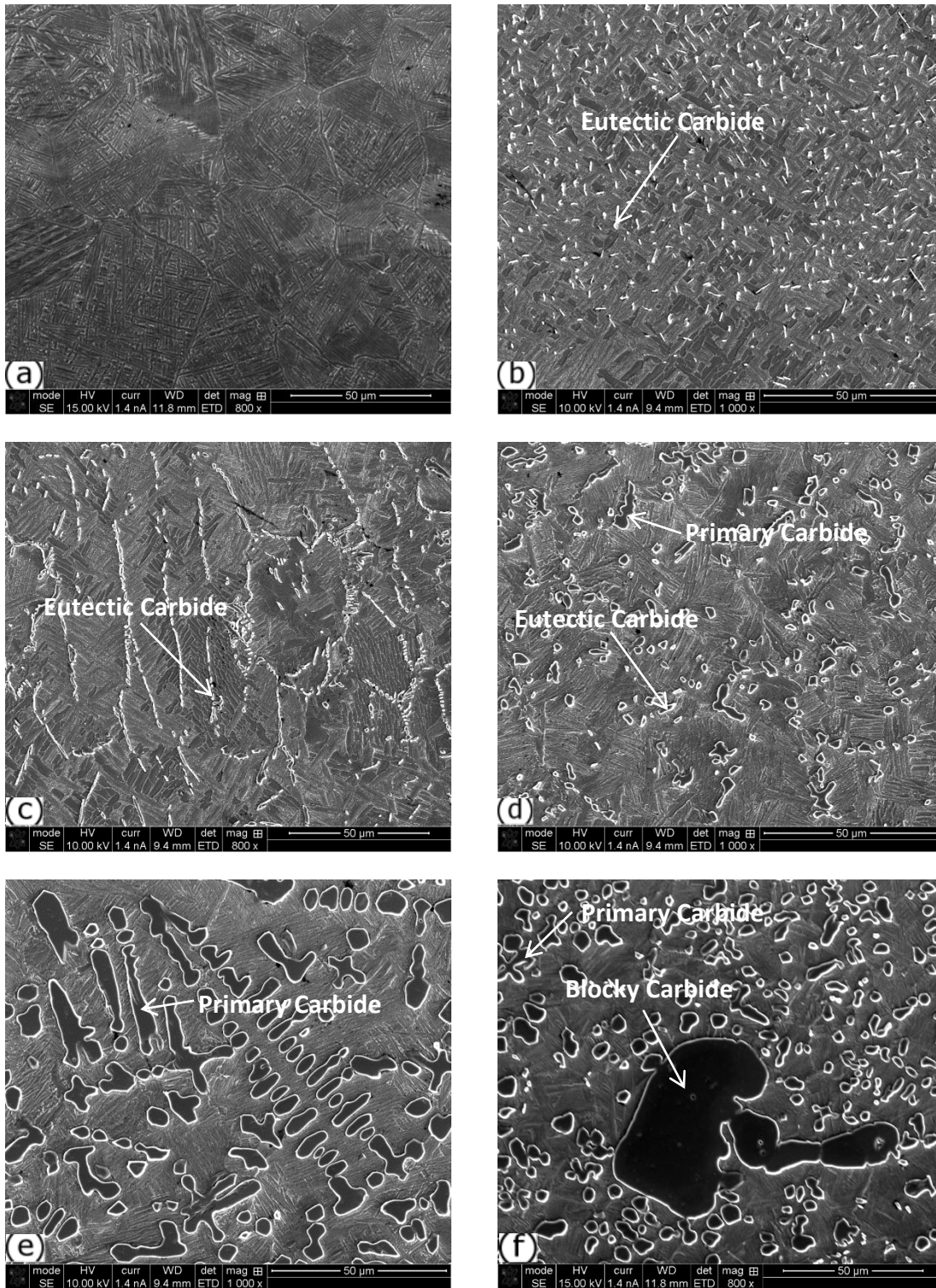


Figure 3. Microstructure of Ti-6Al-4V/TiC FGM deposit: (a)-(f): SEM microstructure with increasing carbon content from 0% to 30% at different locations. The etchant is Kroll's etchant.

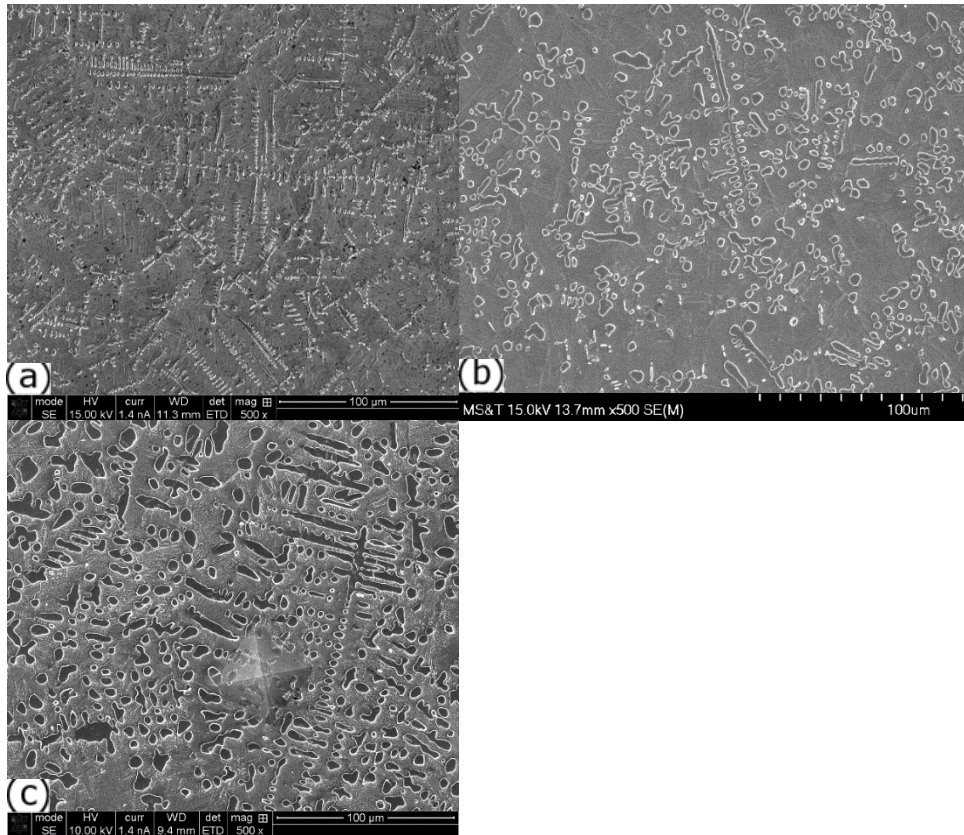


Figure 4. Resolidified carbide microstructure with different laser power: (a) 400W, 300mm/min. (b) 550W, 300mm/min. (c) 700W, 300mm/min. The etchant is Kroll's etchant.

Figure 4 shows the primary and eutectic carbide morphology under different laser power and the same scanning speed (300mm/min). It can be seen that when laser power increases, the primary carbide size becomes larger. The primary dendrite arm spacing (PDAS) of three different laser power are $19.0 \pm 1.2 \mu\text{m}$, $26.1 \pm 5.7 \mu\text{m}$ and $61.9 \pm 15.7 \mu\text{m}$. The average secondary dendrite arm spacing (SDAS) of three different laser power is $1.2 \pm 0.2 \mu\text{m}$, $1.7 \pm 0.2 \mu\text{m}$ and $2.9 \pm 0.5 \mu\text{m}$. The PDAS and SDAS rise because higher laser power results in a lower cooling rate in the solidification process, which provides dendrite with more time to develop and grow.

3.2 Hardness Result

Five deposited samples were tested with Vickers hardness at 1 kg force and 10 second loading time. Figure 5 shows the indentation positions on one of the FGM deposit samples. The Vickers hardness profile is shown in Figure 6 and Figure 7. The lowest hardness value appears in Ti-6Al-4V substrate region, which is 300 HV1. Along the deposition direction, the hardness value increases to approximately 600 HV1 owing to the existence of the increasing content of carbide. The nonlinear increase might be due to the diffusion of carbon and the discrepancy between unmelted carbide hardness and resolidified carbide hardness. When error bars are

incorporated into the Vickers hardness measurement result shown in Figure 6 and Figure 7, three laser power and scanning speed doesn't significantly influence FGM deposit hardness distribution.

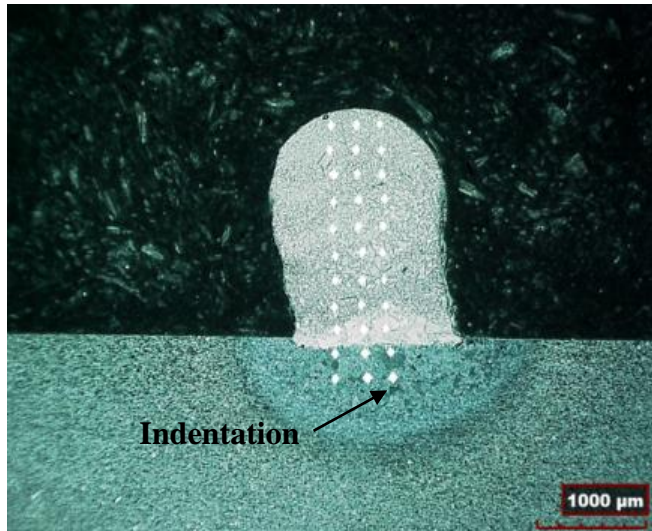


Figure 5. Schematic of Vickers hardness test.

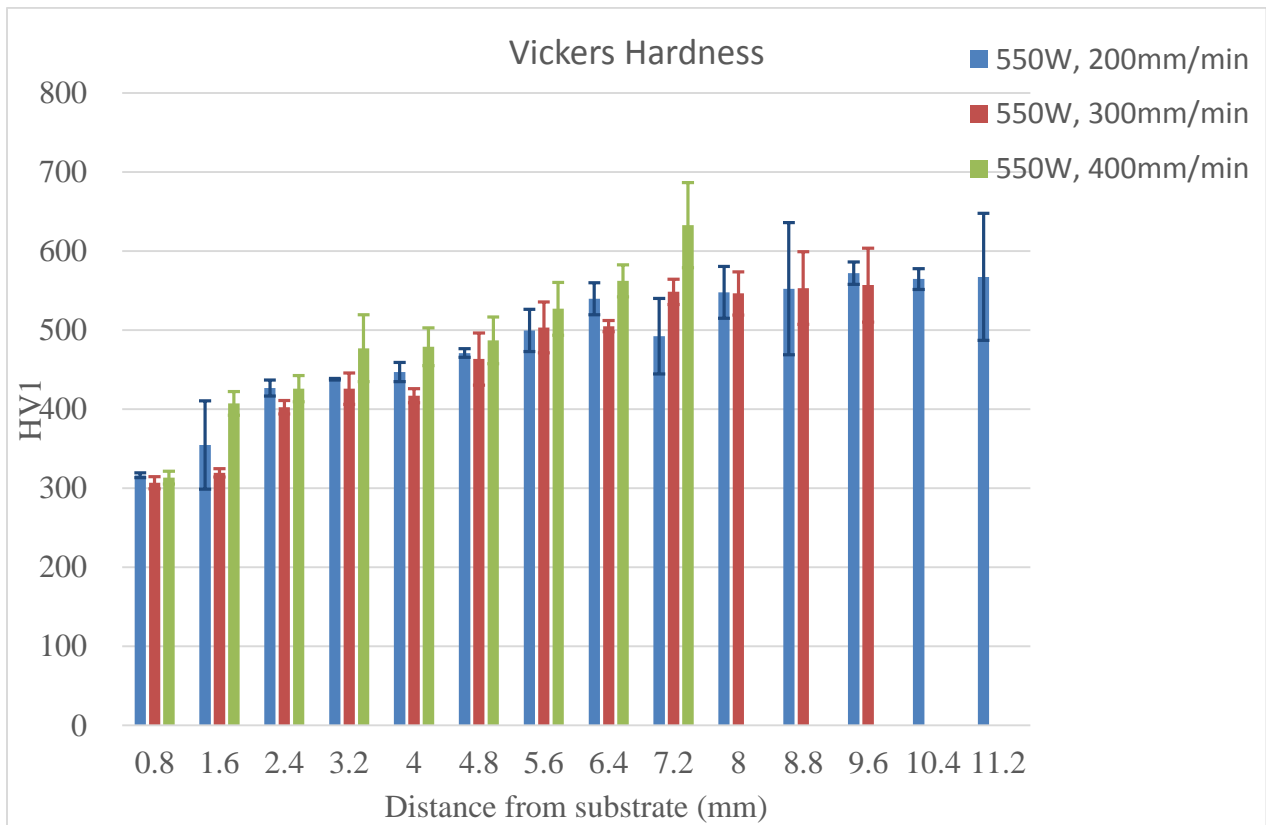


Figure 6. Vickers hardness result from substrate to top deposit at different laser scanning speed

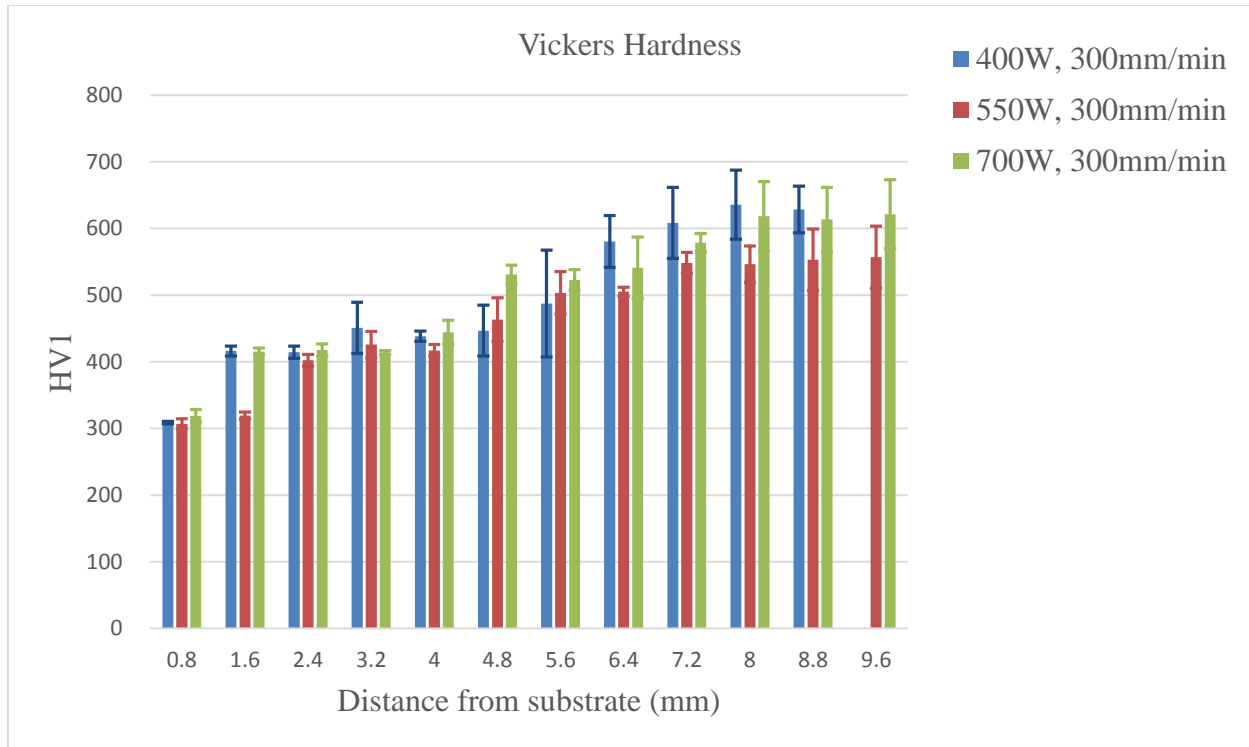


Figure 7. Vickers hardness result from substrate to top deposit at different laser power

3.3 XRD Analysis

Figure 8 shows x-ray diffraction patterns at different locations on the deposit. XRD was able to detect α -Ti (HCP), β -Ti (BCC) and TiC (FCC) phases. An approximately 2mm*2mm area was scanned in the XRD analysis. There is no intermetallic phase identified in the deposit area, which could have caused cracking within the deposit. At the top area of Ti-6Al-4V/TiC deposit, the TiC phase dominates compared to α -Ti and β -Ti, which is agreement with the microstructure and hardness result. Although α -Ti content is higher than β -Ti, there are still some remaining β -Ti due to high cooling rate in the solidification process. Some β phase cannot be transformed to α phase below transus temperature. At the bottom area of Ti-6Al-4V/TiC deposit, α -Ti and β -Ti are the dominant phases.

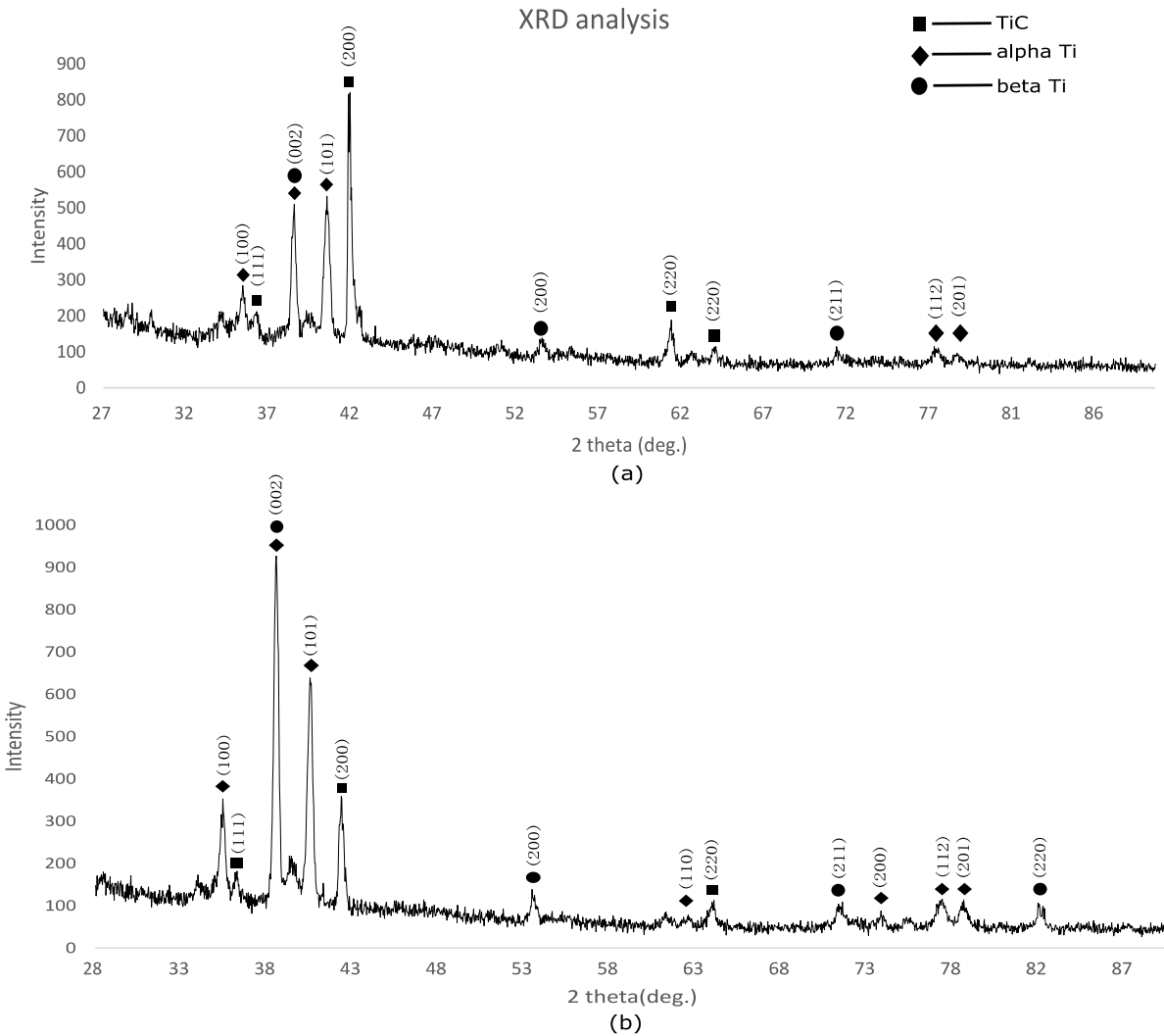


Figure 8. XRD analysis result of deposit area: (a) XRD analysis on top deposit cross section (b) XRD analysis on bottom deposit cross section

4 Conclusion

- 1) Ti-6Al-4V/TiC FGM deposit from 10 vol% to 30 vol% was successfully fabricated by laser metal deposition process with premixed powder. Primary carbide, eutectic carbide and unmelted carbide can be observed at deposit region, and α - Ti, β - Ti and FCC structure TiC can be detected at high and low area in the deposit.
- 2) When laser power rises, the primary and secondary dendrite arm spacing size also increases because the cooling rate is distinctly influenced by laser power.
- 3) The Vickers hardness result will approximately increase from 300VH1.0 to 600VH1.0 from Ti-6Al-4V substrate to top deposit. Three laser power and scanning speed doesn't affect the hardness result significantly.

5 Acknowledgement

This work was funded through NASA's EPSCoR Grant #NNX13AM99A. We appreciate the NASA support.

6 References

- [1] Liu, D., Zhang, S. Q., Li, A., and Wang, H. M., 2009, "Microstructure and tensile properties of laser melting deposited TiC/TA15 titanium matrix composites," *J. Alloys Compd.*, **485**(1–2), pp. 156–162.
- [2] Candel, J. J., Amigó, V., Ramos, J. A., and Busquets, D., 2010, "Sliding wear resistance of TiCp reinforced titanium composite coating produced by laser cladding," *Surf. Coatings Technol.*, **204**(20), pp. 3161–3166.
- [3] Liu, D., Zhang, S. Q., Li, A., and Wang, H. M., 2010, "High temperature mechanical properties of a laser melting deposited TiC/TA15 titanium matrix composite," *J. Alloys Compd.*, **496**(1–2), pp. 189–195.
- [4] Ochonogor, O. F., Meacock, C., Abdulwahab, M., Pityana, S., and Popoola, A. P. I., 2012, "Effects of Ti and TiC ceramic powder on laser-cladded Ti–6Al–4V in situ intermetallic composite," *Appl. Surf. Sci.*, **263**(0), pp. 591–596.
- [5] Mahamood, R. M., Akinlabi, E. T., Shukla, M., and Pityana, S., 2013, "Scanning velocity influence on microstructure, microhardness and wear resistance performance of laser deposited Ti6Al4V/TiC composite," *Mater. Des.*, **50**(0), pp. 656–666.
- [6] Liu, W., and DuPont, J. N., 2003, "Fabrication of functionally graded TiC/Ti composites by Laser Engineered Net Shaping," *Scr. Mater.*, **48**(9), pp. 1337–1342.
- [7] Wang, F., Mei, J., and Wu, X., 2007, "Compositionally graded Ti6Al4V+TiC made by direct laser fabrication using powder and wire," *Mater. Des.*, **28**(7), pp. 2040–2046.
- [8] Obielodan, J., and Stucker, B., 2013, "Characterization of LENS-fabricated Ti6Al4V and Ti6Al4V/TiC dual-material transition joints," *Int. J. Adv. Manuf. Technol.*, **66**(9-12), pp. 2053–2061.
- [9] Liya Regel, W. R. W., 2000, *Processing by Centrifugation*, Kluwer Academic Publishers-Plenum Publishers, New York.